



Physico-chemical and radioactive characterization of TiO₂ undissolved mud for its valorization

M.J. Gázquez^a, J. Mantero^b, J.P. Bolívar^{a,*}, R. García-Tenorio^b, F. Vaca^a, R.L. Lozano^a

^a Department of Applied Physics, University of Huelva, Huelva, Spain

^b Department of Applied Physics II, University of Seville, Seville, Spain

ARTICLE INFO

Article history:

Received 1 March 2011

Received in revised form 15 April 2011

Accepted 17 April 2011

Available online 23 April 2011

Keywords:

NORM industry

Titanium dioxide

Characterization waste

Ilmenite undissolved muds

ABSTRACT

In order to find a potential valorization of a waste generated in the industrial process devoted to the production of TiO₂ pigments, and as an essential and basic step, this waste must firstly be physically and chemically characterized. Moreover, the content of radioactivity is taken in to account due to it comes from a NORM (Naturally Occurring Radioactive Material) industry. With this end, microscopic studies were performed by applying scanning electron microscopy with X-ray microanalysis (SEM–XRMA), while the mineralogical compositions were carried out by means of the X-ray diffraction (XRD) technique. The concentrations of its major elements were determined by X-ray fluorescence (XRF), while heavy metals and other trace elements were ascertained through Inductively Coupled Plasma Mass Spectrometry (ICP–MS).

The results obtained for this waste have revealed several lines of research into potential applications. Firstly, with the refractory properties of mineral phases observed leading to a possible use in the ceramics industry or in thermal isolators. And secondly, attending to the characteristic particle-size spectra can be used as an additive in the manufacture of cement and finally, its high concentration of titanium may be used as a bactericide in brick production.

© 2011 Elsevier B.V. All rights reserved.

1. Introduction

The generation of inorganic waste is an unavoidable consequence of the implementation of industrial production processes using minerals as primary materials, and leads to a series of drawbacks associated to environmental, health and economic issues. Hence, in order to decrease its negative impact on both the environment and health, the efforts towards the recycling or valorization of inorganic wastes generated by different industrial processes has been escalating exponentially over recent years [1–5]. The minimization of waste disposal and preventing its potential release into the environment can generate environmental and economical benefits not only for these industries, but also for the general population [6–8].

Moreover, when the properties of the generated waste render it feasible for use in specific applications, these products can successfully compete with those made from primary materials, thereby further reducing the environmental cost of waste disposal. The appropriate treatment of industrial waste could even lead to the generation of co-products of economic value and broad applica-

tion [9–12]. Obviously, the environmental and health impacts of these co-products must comply with existing regulations.

The production process of titanium dioxide; the most commonly used white pigment usually involves one of two alternative processes, called “chloride” and “sulphate” routes [13–15]. Our study focuses on a titanium-dioxide industry, located in the province of Huelva (Spain), which produces pigments by applying the sulphate process and uses two raw materials as feedstock: ilmenite (FeTiO₃){ILM}, and titaniferous slag {SLAG}. Ilmenite is a heavy mineral containing approximately 43–65% titanium dioxide [16,17], while titaniferous slag, which contains 70–80% titanium dioxide, is a co-product of ilmenite smelting which is carried out in order to decrease the reagent consumption and waste material accumulation in the subsequent pigment-making process. Slag is used to remove (or at least to reduce) the iron input in the titanium-dioxide chemical process, thus obtaining slag high in titanium and marketable iron metal [18–20].

In the Huelva TiO₂ industry, several waste and co-products are generated throughout the process. In particular, and before the valorization of the waste is carried out, an exhaustive and complete physico-chemical analysis is crucial in order to discover its most suitable applications. The examination must be completed with a detailed radiological characterization since the TiO₂ industry is considered a NORM industry. Ilmenite, presents enhanced levels of

* Corresponding author. Tel.: +34 959 218010; fax: +34 959 219777.

E-mail address: bolivar@uhu.es (J.P. Bolívar).

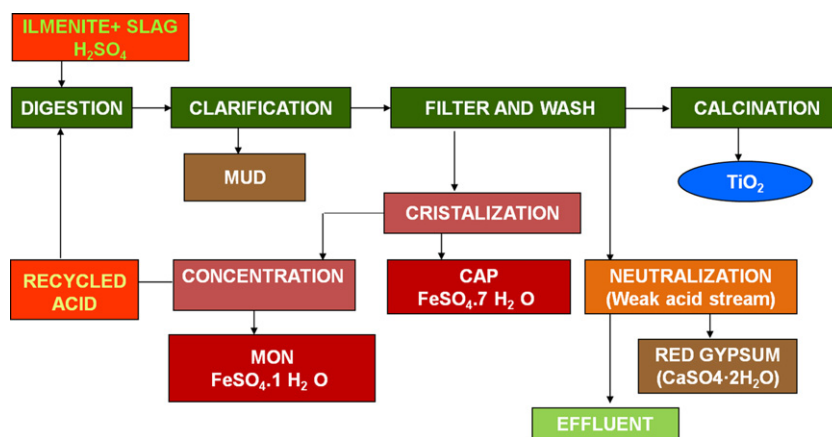
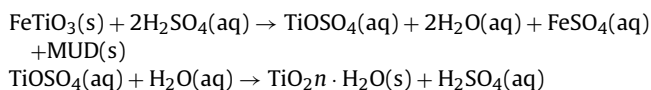


Fig. 1. Diagram of the sulphate process used in the Huelva factory.

radionuclides from the natural uranium and thorium series. Some of these radionuclides can be found enriched in the waste under study.

The main steps in the TiO_2 production process at the Huelva factory are set out in Fig. 1, and described in the following paragraphs. The process starts with a digestion process where a blend of ilmenite and slag is mixed with highly concentrated sulphuric acid (80–95%). A highly exothermic reaction for the digestion of the feedstock containing TiO_2 is initiated by the addition of water and recycled acid.

The digestion process can be summarized as:



The resulting liquor contains titanyl sulphate (TiOSO_4) and iron sulphate (FeSO_4) dissolved in sulphuric acid. To ensure that all the Fe is in dissolution, the liquor is passed through scrap metal (Fe reduction step).

The generated reduced liquor is passed then to a clarification tank where the undissolved solids, called mud, are allowed to settle; the mud is then separated from the solution by flocculation (decantation) and filtration. Until now, this mud has been neutralised and, finally, disposed of in a controlled disposal area, since no economically sound application had been found. This undissolved mud is highly acid, and consists of a number of metals that can adversely affect the environment if they are not managed adequately. The disposal of this mud incurs a significant proportion to the cost of the final product of the industrial process, the TiO_2 pigment. In the Huelva factory about 142,000 metric tonnes of raw material are processed (85% ilmenite and 15% slag), with the resulting generation of 30,000 metric tonnes of mud.

After separation of the mud, the precipitation of the hydrated TiO_2 from the clarified reduced liquor is achieved by boiling it for several hours followed by cooling. The precipitated TiO_2 is then separated by vacuum filters (called “Moore filters”) from the mother liquor (“strong” acid, 20–25% H_2SO_4) and washed with water in order to remove the remaining impurities. Finally, the washed TiO_2 pulp is placed in rotary kilns for the removal of its water content and traces of sulphur. The resulting solid is calcined and finely ground (“micronized”), before being packed for commercial distribution.

With respect to the mother liquor which remains after the precipitation of the TiO_2 , it is important to mention that this cannot be considered as a waste of the process since it is treated for the generation of a “clean” acid which is recycled in the process. Several co-products, such as copperas (ferrous sulphate heptahy-

drate, $\text{FeSO}_4 \cdot 7\text{H}_2\text{O}$), and sulfafer (ferrous sulphate monohydrate, $\text{FeSO}_4 \cdot \text{H}_2\text{O}$) which have established markets [15,17] have been obtained in recent years.

This paper focuses on the physico-chemical and radioactive characterization of a specific waste (undissolved ilmenite mud) generated in industries devoted to titanium-dioxide production, as an essential step in the pursuit for realistic applications of this waste.

2. Materials and methods

2.1. Materials

The samples of raw materials (ilmenite and slag) and waste (mud) used in this study have been collected from a titanium-dioxide production plant located 12 km from the city of Huelva, in southwest Spain. Five sampling campaigns were organised for a period of one month, with a sampling taking place every six days, to evaluate the possible temporal variability of the characteristics of this waste. After collection, all samples were dried at 105°C until reaching a constant weight before analysis.

2.2. Methods for physical and chemical characterization

2.2.1. XRD

The mineralogical study is performed by applying the disoriented dust method with a Bruker laser diffraction instrument, and by using the $\text{K}\alpha$ radiation of Cu (filtered by a Ni film) excited by 30 mA of intensity and 40 kV of tension. The mineralogical quantification is carried out using Bruker’s EVA software with internal standard. We point out that this technique is only valid for detecting crystalline compounds.

2.2.2. Chemical analysis

Trace elements have been determined by Inductively Coupled Plasma Mass Spectrometry (ICP-MS) by using an HP4500® system at the Research Central Services, in the University of Huelva, with the followings analytical parameters: RF generator to 1350 W, carrier gas 1.15 L/min, nebulizer pump 0.12 rps, sampling depth 6.2 mm, Bias Omega lens –27 V, Omega minus lens –7 V and extraction lens 1, –171 V. To this end, representative aliquots (0.2 g) of the samples to be analysed are subjected to a hard acid attack until near total dissolution. The digestion method has been carried out by using 3 mL of 65% HNO_3 , 1 mL of 37% HCl and 8 mL of 40% HF . After the evaporation to the resulting solution, 10 mL of HClO_4 is added and the solution is again evaporated. The digestion process is completed with another final acid attack with 10 mL of HNO_3 , and

this is evaporated to dryness. Finally, was diluted and prepared for introduction into the measuring system in 2% nitric acid.

The major elements are measured for X-ray fluorescence (XRF) with a Bruker S4 Pioneer system which has the following characteristics: 4 kW, front window and anode of Rh; five analysing crystals; LIF200, Ge, PET, OVO55 and OVOC, and two X-ray detectors. This technique requires the samples under analysis to be as homogeneous as possible. For this reason, in our case 1 g aliquot of each dry sample is taken and mixed with 10 g of lithium tetraborate (material used for melting), with 5 drops of lithium iodine at 20%. Each mixture is placed in a crucible of Pt–Au, which is introduced into a special furnace for its fusion. The final result for each sample is a homogenous glass, called “pearl”, ready to be measured.

2.2.3. Granulometry

Granulometry analyses are achieved by using the Mastersize 2000 APA 2000 model (©Malvern Instruments Ltd.). For a precise granulometric measurement, a representative amount of each sample is placed in water for 24 h to achieve a high level of disintegration of the original matrix. For a correct homogenization of the matrix, each sample is then introduced into a magnetic separator at a constant speed of 700 rotations per minute, and from here aliquots are collected by the Mastersize 2000 system for their analysis.

2.2.4. Scanning electron microscopy (SEM) with X-ray microanalysis

The scanning electron microscope is a type of electron microscope that creates an image of the sample surface by scanning it with a high-energy beam of electrons in a raster-scan pattern. The electrons interact with the atoms constituting the sample, thereby producing signals that contain information about the surface topography, composition and other properties of the sample, such as its electrical conductivity. The SEM analyses are carried by using a JEOL JSM-5410 system, working at 20 kV. It has a backscattered electron detector (BSE), by Tetra Link of Oxford, and a dispersive X-ray spectrometer for EDS (energy-dispersive X-ray spectroscopy).

2.2.5. Alpha and gamma spectrometry

The radioactive characterization of all the samples is performed by applying two independent techniques: gamma-ray and alpha-particle spectrometry. Gamma measurements were carried out by using a gamma spectrometry system, which has 38% relative efficiency and FWHM of 0.95 keV at the 122 keV line of ^{57}Co , and of 1.9 keV at the 1333 keV line of ^{60}Co . The complete procedure of calibration of this gamma spectrometry system is described elsewhere [21].

Th- and U-isotope activity concentrations are determined by alpha-particle spectrometry in aliquots of the samples analysed. For the determination of these isotopes, a well-established sequential radiochemical method is applied [22] in order to first place them in dissolution and later to isolate the radionuclides of interest. Due to the very low solubility of the raw materials and the muds, a total-dissolution method is applied based on KHSO_4 , as previously validated by our group [23]. After isolation, the U and Th isotopes were electrodeposited independently onto stainless steel discs, which were measured in an EG&G Ortec alpha spectrometry system.

3. Results and discussion

3.1. Mineral composition

Information on the mineralogical composition of the raw materials (ILM and SLAG) and of the undissolved mud (MUD) determined

Table 1

Average (of 5 samples) mineralogical composition (%) of raw materials and mud in the Huelva TiO_2 industry. Uncertainties are given as 1σ (standard deviation). N.D. No detection.

	ILM	SLAG	MUD
Ilmenite (FeTiO_3)	71 ± 11	N.D.	22 ± 3
Rutile (TiO_2)	7.0 ± 2.4	8.4 ± 2.4	34 ± 4
Pseudo-rutile ($\text{Fe}^{3+}_2\text{Ti}_3\text{O}_9$)	20 ± 7	N.D.	N.D.
Armalcolite ($(\text{Mg,Fe}^{2+})\text{Ti}_2\text{O}_5$)	N.D.	91 ± 3	N.D.
Zircon (ZrSiO_4)	N.D.	N.D.	12.1 ± 2.0
Quartz (SiO_2)	N.D.	N.D.	13 ± 3
Fe, and Ti oxides ($\text{Fe}_3\text{Ti}_3\text{O}_{10}$)	N.D.	N.D.	18.0 ± 1.9

by XRD is compiled in Table 1. In the ilmenite samples, the following species, remain dominant: ilmenite (FeTiO_3), rutile (TiO_2) and pseudo-rutile ($\text{Fe}^{3+}_2\text{Ti}_3\text{O}_9$), while the slag samples present a main mineralogical composition called armalcolite ($(\text{Mg,Fe}^{2+})\text{Ti}_2\text{O}_5$), around 90%, and about 8.4% of rutile (TiO_2). The uniformity in the mineralogical composition of the slag samples analysed is very high. This constitutes no cause for surprise if the process of generation of this material is taken into account. The titanium slag is an intermediate product made from ilmenite where, the iron oxides are reduced to metallic iron, thereby producing a TiO_2 -rich slag [19,20].

In the mud samples, several species are observed: ilmenite and rutile, with a percentage of 22% and 34%, respectively, and additionally some new previously undetected, such as zircon (ZrSiO_4), quartz (SiO_2), and Fe and Ti oxides ($\text{Fe}_3\text{Ti}_3\text{O}_{10}$), see Table 1. The high percentage of rutile and the detection and quantification in the mud of the aforementioned new mineral phases (zircon and quartz) cannot be considered as surprising, since all of these species are insoluble in sulphuric acid [15]. This reading simply reflects a concentration effect, since for each unit of dry raw material entering the process, 0.16 units of wet mud is obtained, which contains around 40% humidity (0.10 units of dry mud).

The main mineralogical characteristic of the mud samples is that all their mineralogical phases are highly refractory. This fact reveals perspectives for the analysis of its possible use in several applications, for example, as an additive in the ceramic industry [24,25]. Furthermore, this material, due to its refractory character, should be a very good thermal isolator and applications can be found linked to this property.

3.2. Major elements

In Table 2, the average concentrations (%) are compiled, as obtained for the major elements in the analysis of the five mud samples collected in the industrial process of TiO_2 production over a period of approximately a month. In the same table, and for comparison purposes, the average concentrations of the same elements associated to the raw material are also compiled.

As expected, the major elements in the raw material are Fe and Ti, 39% and 53.8%, respectively [16], indicating their associated low uncertainties the high uniformity found in the five samples analysed. The mud samples, in addition to Fe and Ti, contain appreciable and relatively uniform levels of different metals, like Si, Al, Mn, Mg and Ca, (all expressed in Table 2 as oxides).

It is important to point out the high average concentration of titanium oxides (51%) found in the mud samples, which represent about 5% of the total concentration of titanium content in the raw material. This fact open doors for the application of several methods for the recovery of a proportion of the titanium remaining in the mud, and also for the possible use of the mud generated in the TiO_2 industry as bactericide coatings in the manufacture of bricks [26,27]. Moreover it contains appreciable amounts of iron and silicon oxides, 13.7% and 16.8%, respectively, (data consistent with

Table 2
Concentration (%) of major elements in samples of waste (MUD). (Uncertainties are given as 1σ (standard deviation). R.M. indicates the average concentration of raw material (85% ilmenite and 15% slag).

	MUD 1	MUD 2	MUD 3	MUD 4	MUD 5	Average	R.M.
SiO ₂	19.18	15.94	14.89	17.49	16.67	16.8 ± 1.6	0.98 ± 0.27
Al ₂ O ₃	3.99	3.46	3.12	3.79	3.55	3.6 ± 0.3	0.95 ± 0.18
Fe ₂ O ₃	14.48	14.87	13.11	12.99	12.91	13.7 ± 0.9	39.0 ± 1.7
MnO	0.48	0.47	0.43	0.43	0.43	0.45 ± 0.02	1.14 ± 0.09
MgO	1.31	1.37	1.29	1.35	1.31	1.33 ± 0.02	1.04 ± 0.15
CaO	0.74	0.77	0.7	0.7	0.66	0.71 ± 0.03	0.13 ± 0.03
TiO ₂	50.09	51.17	52.92	51.55	50.46	51.2 ± 1.1	53.8 ± 0.9
SO ₃	5.24	8.87	6.11	5.36	5.14	6.1 ± 1.6	<0.01

the mineralogical composition, Table 1). In fact, practically all silicon oxides present in the raw material finish associated to the mud samples, due to the concentration factor. Furthermore, the mud contains non-negligible concentrations of different metals such as Al, Mg, Ca, and Mn. The concentration of S (expressed as SO₃) is approximately 6%, which is unsurprising if we consider that the mineral digestion where the mud is generated is carried out with concentrated sulphuric acid [17].

3.3. Trace elements

Trace element concentrations for each sample of mud analysed, together with the average concentrations found for the same elements in the raw material, are compiled in Table 3. For comparison purposes, the same table also shows the average concentrations of the same elements which can be associated to a typical soil (continental crust composition) since the waste (mud) under analysis can reach through their potential applications the environment, and the levels of metals and other compounds from the samples should not greatly exceed those found in uncontaminated soils in order to assure minimal environmental impact. To this end, for each element an “enrichment factor” defined as the ratio between its average concentration in the mud samples and its average concentration in a typical soil has been calculated, and the results obtained are also included in Table 3.

In the aforementioned Table it is observed that trace element concentrations for the raw material samples are relatively uniform, and only average values are presented. The Co and Cd concentrations are a factor of approximately 3–4 times higher in the raw material than in mud, while other elements, such as Cr, Cu, As, Pb, and U, present clearly lower concentrations in the raw material. On the other hand, most trace elements analysed in the mud samples, such as V, Cr, Zn, As, Cd, and Pb, show high enrichment factors: 10, 6, 3, 12, 7 and 16, respectively, in relation to a typical soil, see Table 3. The enrichment factor found for Zr (90) is particularly high, with concentrations in the mud samples ten times higher than in the

raw material, in agreement with the calculated concentration factor (remember that 1 g of ilmenite generates 0.10 g of dry muds). This indicates that all Zr originally present in the raw material, ends up associated to the mud samples; a fact which remains unsurprising in view of the mineralogical results, see Table 1. It is also interesting to point out that the concentration of Th in the mud samples is high, with values of 70 mg/kg, 6–7 times higher than a typical soil, but lower than the concentration found for the raw material. At the same time, the concentration of U in mud is relatively high, 7 times higher than in undisturbed soils, and higher, by a factor of 2–3, than in the raw material.

3.4. Granulometry

The knowledge of the grain-size distribution for the mud samples analysed in this work can be considered essential for the discovery of potential applications, since most of their physical and chemical properties depend on the magnitude of the particle size spectrum of its grains. The granulometric results of the five mud samples are compiled in Table 4 and shown in Fig. 2. From these data, it can be observed immediately that the five samples analysed can be classified into two groups with three well-defined zones in the particle-size spectrum.

The first group consists of samples 1, 2 and 4, characterized as presenting high concentration of clay (36% < 4 μm), and silt (18% in the interval 32–63 μm) with a well-defined bimodal particle-size spectrum, while the second group, formed with samples 3 and 5, presents a low concentration of clay (7.8% < 4 μm) and maximum concentration (27%) in the interval 32–63 μm, with a well-defined modal particle-size spectrum. In addition, the proportion of particles of a large size (>63 μm) is clearly higher in the second group of samples: a fact that provokes interest of a practical nature since it may be highly beneficial in its potential use as an additive in the manufacturing of cement [12,29].

It is clear then that the grain particle sizes of the samples belonging to the first group are smaller than those found in the second

Table 3
Average composition of trace elements (mg/kg) in the raw materials and waste analysed. (*) Continental crust composition [28]. R.M. indicates the average concentration of raw material (85% ilmenite and 15% slag). E.F. represents the enrichment factor (concentration in average composition of mud/concentration in continental crust composition).

	MUD 1	MUD 2	MUD 3	MUD 4	MUD 5	Average	R.M.	E.F.	Soil (*)
V	1012.1	895.3	896.7	1003.0	895.8	941 ± 60	1270 ± 90	9.7	97
Cr	582.1	454.6	499.2	557.6	496.4	520 ± 50	46 ± 14	5.7	92
Co	20.6	15.1	14.4	16.1	14.7	16 ± 2.6	52 ± 12	0.9	17
Ni	16.1	12.9	12.8	10.8	12.3	13.0 ± 1.9	14 ± 4	0.3	47
Cu	286.1	257.6	285.4	262.3	299.6	278 ± 18	40 ± 12	9.9	28
Zn	226.1	183.2	178.0	201.9	177.5	193 ± 21	260 ± 50	2.9	67
As	68.6	43.2	66.6	56.2	51.4	57 ± 11	19 ± 4	11.9	4.8
Zr	18010	18750	15900	17280	16160	17200 ± 1200	1300 ± 300	89.1	193
Cd	0.74	0.44	0.58	0.64	0.62	0.60 ± 0.11	2.6 ± 0.7	6.7	0.09
Ce	296.4	257.5	261.4	347.3	274.6	290 ± 40	154 ± 19	4.6	63
Sn	72.5	60.5	90.8	70.0	76.2	74 ± 11	21 ± 6	35.2	2.1
Pb	286.5	265.5	289.9	290.9	257.4	278 ± 16	120 ± 22	16.4	17
Th	75.2	62.7	63.3	81.8	66.2	70 ± 8	83 ± 17	6.4	11
U	20.0	17.6	19.3	18.3	17.4	18.5 ± 1.1	6.5 ± 1.3	6.9	2.7

Table 4

Average grain-size composition (%V) of the five mud samples.

Size (microns)	Type	MUDS samples 1,2 and 4		MUDS samples 3 and 5	
		Average concentration	Global	Average concentration	Global
<4	Clay	36 ± 5	36 ± 5	7.8 ± 2.8	7.8 ± 2.8
4–8	Silt	11 ± 3	55 ± 3	4.3 ± 1.0	54 ± 3
8–16		9 ± 1		7.1 ± 0.3	
16–32		17 ± 1		16 ± 1	
32–63		18 ± 1		27 ± 3	
63–125	Sand	7.8 ± 1.6	9 ± 2	25 ± 3	38 ± 4
125 – 250		0.4 ± 0.5		11.8 ± 0.1	
250–500		0.3 ± 0.6		1.5 ± 2.1	
500 – 1000		0.5 ± 0.8		0.06 ± 0.08	
1000–2000		0.00		0.00	

group, a fact that may constitute an indication that their generation processes could be slightly different. In this sense, we must remember that in the production process the liquor containing titanylsulphate and iron pass through a clarification tank, where the undissolved solids (muds) are separated from the solution in two processes, first by decantation (coarser grains), and then by filtration (smaller grains). The granulometric data indicates that the samples belonging to the first group should mainly include those whose mud is separated in the filtration step, while the second group should be made up of samples of mud separated by flocculation and/or decantation.

3.5. Scanning electron microscopy

Highly relevant information on the morphology of the mud samples, and in particular about their particle-size distribution, texture and porosity of the materials, is gained by applying the scanning electron microscopy technique with energy-dispersive X-ray spectroscopy (EDX).

A representative SEM image, corresponding to one of the mud samples analysed in this work, is shown in Fig. 3, and it is possible to observe that the mud is composed of particles of very heterogeneous sizes (which mainly oscillate between 4 and 63 μm , in agreement with the granulometry results). In addition, the analysis by EDX indicates that, this sample is mainly composed of Si and Ti, with other elements such as Fe, Mn, and Al, found in trace concentrations, although the composition of individual particles is quite heterogeneous. This information is in agreement with the results obtained previously by means of XRF, Table 2.

Furthermore, in the SEM image of Fig. 4, a total of 5 different marked particles can be observed with a similar size, of approximately 50 microns, although they present a non-uniform composition. The EDX analyses associated to Fig. 4 indicate that the particles marked with the numbers 2 and 3 are quartz crystals with impurities of Ti, Ca, Fe and Al, while particle 4 is an ilmenite crystal (FeTiO_3), and particle 1 is zircon (ZrSiO_4). Finally, particle 5 exhibits a very uniform composition, where the Ti appears as main element, which indicates that is rutile (TiO_2) with traces of Fe, Al, and Si. These results are to be expected since they agree with the

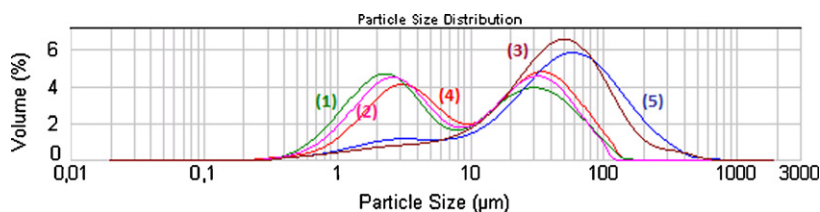
mineralogy and composition previously determined by XRD and XRF.

In relation to the morphology of the mud samples, laminar crystals of less than 50 microns have been observed by means of SEM, in addition to the dominant pseudo-tabular morphology, similar to that of ilmenite crystals [17].

Moreover, when backscattered electron images of the mud samples were generated, the presence of some shiny microscopic particles was detected, indicating the presence of elements with high atomic number. An EDX spectrum analysis of these shiny particles gives a typical heavy metal mineral composition (Ce, Th, and other REE), as can be observed in Fig. 5. The presence of these heavy elements and REE in the mud samples might be associated to the monazite mineral phase. This presence was known before the SEM studies since in the previously performed chemical analyses, being detected in non-negligible amounts, see Table 3.

3.6. Radiological concentrations

Table 5 shows the average activity concentrations of several natural radionuclides belonging to the uranium and thorium series, whose half-lives are longer than one month. These concentrations were determined thorough radiometric analyses in the samples of ilmenite {ILM}, slag {SLAG}, and waste {MUD}. It can first be observed that all the values associated with the mean deviations fall below 16%, which indicates that the samples show high homogeneity with respect to the radioactivity. It is also possible to confirm that ilmenite is a NORM mineral since it is enriched in natural radionuclides from both Th and U series (in secular equilibrium), with a total concentration of 440 Bq/kg for ^{238}U and ^{232}Th nuclides. On the other hand, it can be observed that the radionuclide levels for slag are lower than those found in typical undisturbed soil (35 and 30 Bq/kg for ^{238}U and ^{232}Th , respectively) [30]. Therefore, the use of this material in the production process, has a positive radiological effect. However, the activity concentrations in the mud samples are far from negligible, which implies that this waste should also be considered and treated as a NORM. The mud contains a total concentration of radionuclides greater than 1 Bq/g [31], which is a considerable fraction of the radioactivity content originally present

**Fig. 2.** Particle-size distribution (%V) of five mud samples.

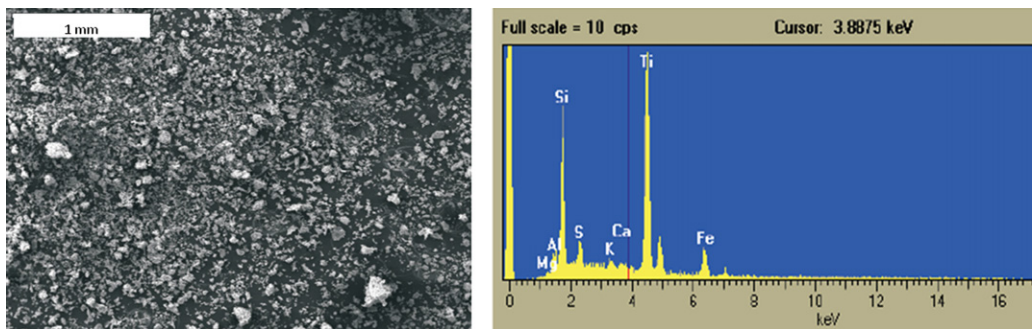


Fig. 3. SEM image of one mud sample (secondary electron mode) and its corresponding representative EDX spectrum.

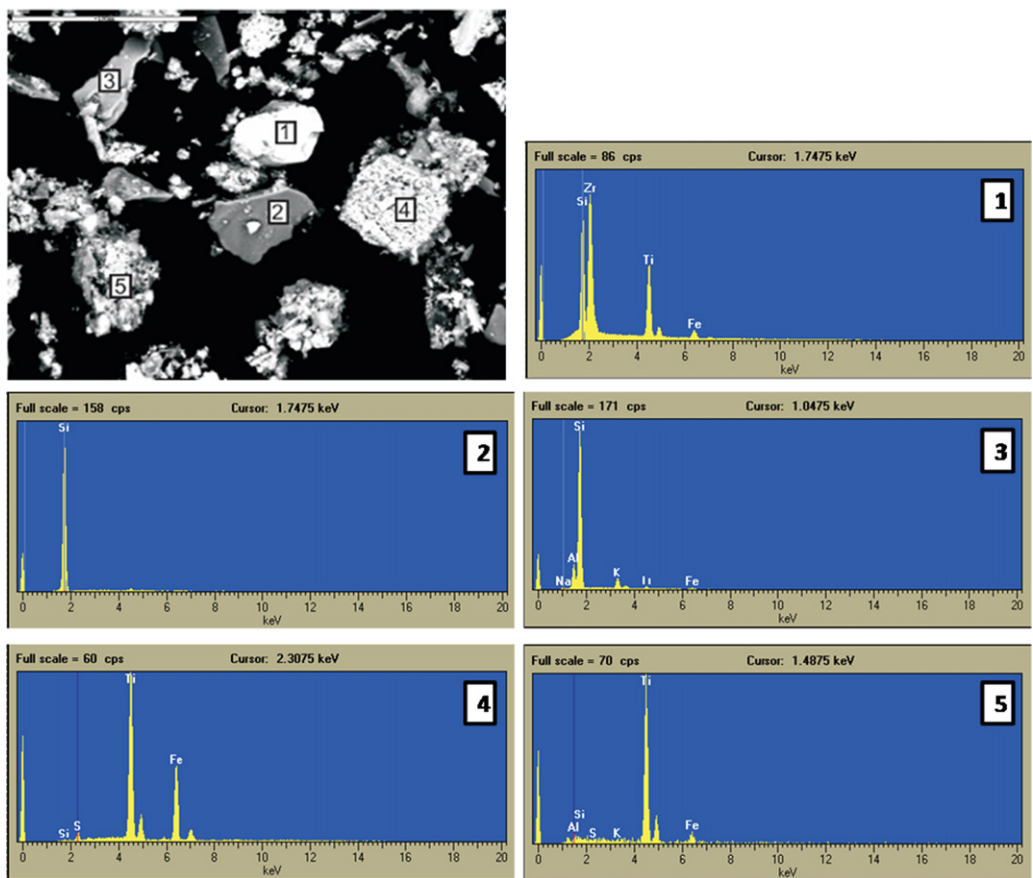


Fig. 4. SEM specific analysis of various mud particles by secondary electrons and their corresponding X-ray spectrum.

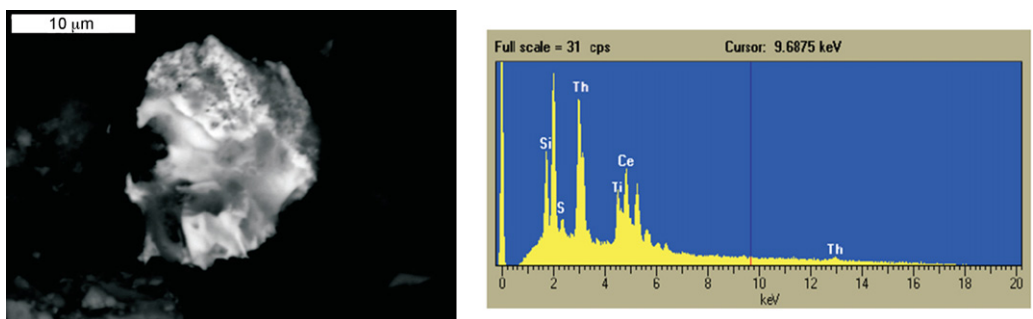


Fig. 5. SEM-EDS specific analysis of one mud particle.

Table 5
Radionuclide concentrations (Bq/kg) of natural origin of ilmenite, slag, and mud. Uncertainties are given as 1σ . N.D. denotes no detection.

	^{238}U	^{234}U	^{230}Th	^{226}Ra	^{232}Th	^{228}Ra	^{228}Th	^{40}K
{ILM}	119 ± 3	129 ± 5	85 ± 5	86 ± 5	315 ± 20	301 ± 20	305 ± 23	20.2 ± 2.2
{SLAG}	5.9 ± 0.7	6.4 ± 1.3	19 ± 4	6.5 ± 0.7	14 ± 3	9.0 ± 1.2	9.8 ± 1.7	N.D.
{MUD}	210 ± 30	240 ± 22	45 ± 3	820 ± 30	350 ± 30	2584 ± 60	680 ± 30	284 ± 11

in the raw materials. In fact, by taking the activity concentration determined in the mud samples, Table 5, and normalizing it by a mass factor (1 part of ilmenite produces 0.10 parts of dry mud), it is possible to deduce that practically all the radium present in the raw material is associated to the mud sample. This fact can be explained by taking into account the insolubility of radium as sulphate [32], which is the existing medium in the digestion step (concentrated sulphuric acid). The ^{228}Ra concentration in the mud sample is approximately 2500 Bq/kg, which is about 100 times higher than those found in typical soils. On the other hand, the concentrations of thorium and uranium in the mud samples represent a low proportion of the concentration present in the ilmenite, since Th and U are soluble elements in sulphuric acid, and they therefore flow through the industrial process attached to the liquor (mainly formed by strong sulphuric acid) from the digestion step. In order to provide a full explanation of the results compiled in Table 5 for the mud samples, it is necessary to emphasise that the secular equilibrium, which originally existed in the mineral in the U- and Th-series radionuclides is broken when is chemically treated with concentrated sulphuric acid. This explains, for example, why the concentration of ^{228}Th (680 Bq/kg, and half life = 1.9 y) is 2 times higher than ^{232}Th (350 Bq/kg) in the mud samples, even though ^{232}Th and ^{228}Th are isotopes of the same element (and therefore have the same behaviour during the industrial process), belong to the same radioactive series, and for that they will be in secular equilibrium in the raw material. The difference in the levels is due to the high initial concentration of ^{228}Ra in the mud in relation to the ^{228}Th one. This ^{228}Ra decays over time and increases the concentration of ^{228}Th activity over the concentration of ^{232}Th until secular equilibrium ^{228}Th - ^{228}Ra is reached (in around 8 years). The radioactive content of the mud samples introduces the question of whether this waste can be valorized as building material. To this end, several international organizations propose reference values for the natural radionuclide concentrations in building materials. Publication No. 112 [33], from the monographic collection "Radiation Protection" issued by the European Union, defines an external risk index (I), also called an activity concentration index, Eq. (1), to ensure that external gamma dose rates inside a room from building materials does not exceed 1 mSv per year.

$$I = \frac{C(^{226}\text{Ra})}{300} + \frac{C(^{228}\text{Ra})}{200} + \frac{C(^{40}\text{K})}{3000} \quad (1)$$

where $C(^{226}\text{Ra})$, $C(^{228}\text{Ra})$, and $C(^{40}\text{K})$ are the activity concentrations for ^{226}Ra , ^{228}Ra , and ^{40}K , respectively, in the building material considered, expressed in Bq/kg.

This index should not exceed the value $I \leq 1$ for materials used in bulk amounts, e.g. concrete, or $I \leq 6$ for superficial materials and those with restricted use, e.g. tiles, boards, etc., to insure that the additional external dose received by occupants living in buildings constructed with these materials do not exceed the reference value of 1 mSv/year. If the external risk index (I) for the mud samples is calculated using Eq. (1), together with the results compiled in Table 5, a value of approximately 16 is attained. This value is higher than other waste currently used in building materials. For example, in the phosphogypsum the index is in the interval 2.4–3.5 [34], in the blast furnace slag is 1.3–9.1, in the coal fly ash is 1.3–5.7 [35] and in the red mud the interval is around 1.2–3.6 [36]. In this sense, the mud waste has a limited potential use as a building material, and

hence the proportion of this mud within its various applications must be controlled.

4. Conclusions

The present work has been focused on the characterization of a waste (undissolved mud) generated by the titanium-dioxide industry in an effort to study their elemental composition (major, minor and trace elements), granulometry, mineralogy, microscopic morphology, and radioactive content. The main objective is to increase the knowledge about this industrial waste in order to find it potential applications.

Physico-chemical characterization of the raw materials used in the titanium dioxide industry has been carried out in order to evaluate their possible variations in the physico-chemical composition over time and to study the influence of these possible variations in the characteristics of the waste obtained. Our results indicate that the raw material used in the industrial process (ilmenite + slag) has a uniform mineralogical and elemental composition. This fact directly affects the stability and composition of the mud waste and hence its possible valorization.

Furthermore, we have concluded that the waste generated in the industrial process under analysis, undissolved mud, has a very stable composition and that it is formed by refractory species, a fact that paves the way for this material to be used as a thermal insulator. On the other hand, the characteristics of its granulometric spectra, enables this co-product to also be considered as a potential candidate compound for several applications in the manufacture of cement, although, due to its radiological composition, this waste can only be used as a building material after dilution. The main health risk in using this waste in building materials is its high content in radium isotopes, especially in ^{228}Ra : a fact that emphasises the need to include a radiological evaluation of the various materials manufactured with this waste.

Finally, the characterization studies of this waste indicate the presence in its composition of a significant concentration of titanium dioxide (51%), which reveals the necessity for the industrial process to be refined and improved so that the TiO_2 contained in the mud can be recovered.

Acknowledgments

This work has been supported by the PROFIT Project "Valorization of red gypsum from the industrial production of titanium dioxide" (CIT-310200-2007-47), and the Excellence Project of the Junta of Andalucía Government "Modeling and characterization of the phosphogypsum stacks located at Huelva (Spain) for its management and environmental control" (RNM-6300).

References

- [1] T. Kuryatnyk, C. Angulski da Luz, J. Ambroise, J. Pera, Valorization of phosphogypsum as hydraulic binder, *J. Hazard. Mater.* 160 (2008) 681–687.
- [2] P. Colombo, G. Brusatin, E. Bernardo, G. Scarinci, Inertization and reuse of waste materials by vitrification and fabrication of glass-based products, *Curr. Opin. Solid State Mater. Sci.* 7 (2003) 225–239.
- [3] L. Ajam, M. Ben Ouezdou, H. SfarFelfoul, R. El Mensi, Characterization of the Tunisian phosphogypsum and its valorization in clay bricks, *Constr. Build. Mater.* 23 (2009) 3240–3247.

- [4] M. Samara, Z. Lafhaj, C. Chapiseau, Valorization of stabilized river sediments in fired clay bricks: factory scale experiment, *J. Hazard. Mater.* 163 (2009) 701–710.
- [5] Y. Liu, C. Lin, Y. Wu, Characterization of red mud derived from a combined Bayer Process and bauxite calcination method, *J. Hazard. Mater.* 146 (2007) 255–261.
- [6] F. Puertas, I. García-Díaz, M. Palacios, M.F. Gazulla, M.P. Gómez, M. Orduña, Clinkers and cements obtained from raw mix containing ceramic waste as a raw material. Characterization, hydration and leaching studies, *Cem. Concr. Comp.* 32 (2010) 175–186.
- [7] E. Deydier, R. Guilet, S. Sarda, P. Sharrock, Physical and chemical characterization of crude meat and bone meal combustion residue: waste or raw material? *J. Hazard. Mater.* B121 (2005) 141–148.
- [8] A. Acosta, M. Aineto, I. Iglesias, M. Romero, J.M. Rincón, Physico-chemical characterization of slag waste coming from GICC thermal power plant, *Mater. Lett.* 50 (2001) 246–250.
- [9] W. Shen, M. Zhou, W. Ma, J. Hu, Z. Cai, Investigation on the application of steel slag fly-ash phosphogypsum solidified material as road base material, *J. Hazard. Mater.* 164 (2009) 99–104.
- [10] M. Campos, F. Velasco, M.A. Martínez, J.M. Torralba, Recovered slate waste as raw material for manufacturing sintered structural tiles, *J. Eur. Ceram. Soc.* 24 (2004) 811–819.
- [11] A. López-Delgado, H. Tayibi, C. Pérez, F.J. Alguacil, F.A. López, A hazardous waste from secondary aluminium metallurgy as a new raw material for calcium aluminate glasses, *J. Hazard. Mater.* 165 (2009) 180–186.
- [12] J.H. Potgieter, K.A. Horne, S.S. Potgieter, W. Wirth, An evaluation of the incorporation of a titanium dioxide producer's waste material in Portland cement Clinker, *Mater. Lett.* 57 (2002) 157–163.
- [13] P.W. Langmesser, H.G. Volz, G. Kienast, Process leading to the production of titanium dioxide pigment with a high degree of whiteness, U.S. Patent 3,760,058. (1973).
- [14] H.Y. Sohn, L. Zhou, The chlorination kinetics of beneficiated ilmenite particles by CO + Cl₂ mixtures, *Chem. Eng. J.* 72 (1) (1999) 37–42.
- [15] G.S. McNulty, Production of titanium dioxide, in: Proceedings of NORM V International Conference, Seville, Spain, 2007, pp. 169–189.
- [16] T. Chernet, Applied mineralogical studies on Australian sand ilmenite concentrate with special reference to its behavior in the sulphate process, *Miner. Eng.* 12 (5) (1999) 485–495.
- [17] M.J. Gázquez, J.P. Bolívar, R. Garcia-Tenorio, F. Vaca, Physicochemical characterization of raw materials and co-products from the titanium dioxide industry, *J. Hazard. Mater.* 166 (2009) 1429–1440.
- [18] P.C. Pistorius, C. Coetzee, Physicochemical aspects of titanium slag production and solidification, *Metall. Mater. Trans. B* 34B (2003) 581–588.
- [19] P.K. Sahoo, R.K. Galgali, S.K. Singh, S. Bhattacharyee, P.K. Mishra, B.C. Mahanty, Preparation of titania-rich slag by plasma smelting of ilmenite, *Scand. J. Metall.* 28 (1999) 243–248.
- [20] M. Pourabdoli, S. Raygan, H. Abdizadeh, K. Hanaei, Production of high titania slag by electro-slag crucible melting (ECSM) process, *Int. J. Miner. Process.* 78 (2006) 175–181.
- [21] J.P. Perez Moreno, E.G. San Miguel, J.P. Bolívar, J.L. Aguado, A comprehensive calibration method of Ge detector for low level spectrometry measurement, *Nucl. Instrum. Methods Sect. A: Accelerators Spectrom. Detectors Assoc. Equip.* 491 (1–2) (2002) 152–162.
- [22] J.M. Oliveira, F.P. Carvalho, Sequential extraction procedure for determination of uranium, thorium, radium, lead and polonium radionuclides by alpha spectrometry in environmental samples, *Czech. J. Phys.* 56 (2006) 545–555.
- [23] J. Mantero, M. Lehitane, S. Hurtado, R. García-Tenorio, Radioanalytical determination of actinoids in refractory matrices by alkali fusion, *J. Radioanal. Nucl. Chem.* 286 (2010) 557–563.
- [24] S. Teixeira, A.M. Bernardin, Development of TiO₂ white glazes for ceramic tiles, *Dyes Pigments* 80 (2009) 292–296.
- [25] M. Dondi, G. Cruciani, E. Balboni, G. Guarini, C. Zanelli, Titania slag as a ceramic pigment, *Dyes Pigments* 77 (2008) 608–613.
- [26] G. Belardi, L. Piga, S. Quaresima, N. Shehu, Application of physical separation methods for the upgrading of titanium dioxide contained in a fine waste, *Int. J. Miner. Process.* 53 (1998) 145–156.
- [27] A. Calabria Juliana, W.L. Vasconcelos, J. Doni Daniel, R. Chater, D. McPhail, A.R. Boccacchin, Synthesis of sol-gel titania bactericide coatings on adobe brick, *Constr. Build. Mater.* 24 (2010) 384–389.
- [28] R. Gao, Composition of the Continental Crust, *Treatise of Geochemistry*, vol. 3, Elsevier, 2003, pp. 1–64, the Crust.
- [29] N. Diamantonis, I. Marinou, M.S. Katsiotis, A. Sakellariou, A. Papanasiou, V. Kaloidas, M. Katsioti, Investigations about the influence of fine additives on the viscosity of cement paste for self-compacting concrete, *Constr. Build. Mater.* 24 (2010) 1518–1522.
- [30] United Nations Scientific Committee On The Effects Of Atomic Radiation (UNSCEAR) (2000). Report of the United Nations Scientific Committee on the Effects of Atomic Radiation, United Nations, New York.
- [31] IAEA (International Atomic Energy Agency). Safety standards series, Application of the Concepts of Exclusion Exemption and Clearance, Safety guide No RS-G- 1.7. August 2004. STI/PUB/1202.
- [32] R. Landa Edward, Naturally occurring radionuclides from industrial sources: characteristics and fate in the environment, *Radioact. Environ.* 10 (2007), ISSN: 1569–4860.
- [33] European Commission, Directorate-General Environment, Radiation Protection 122 Guidance on General Clearance Levels for Practices, Recommendations of The Group of Experts Established Under The Terms of Article, 31 of the Euratom Treaty, 2000.
- [34] J.L. Aguado, J.P. Bolívar, E.G. San Miguel, R. García-Tenorio, Ra and U isotopes determination in phosphogypsum leachates by alpha-particle spectrometry, *Radioact. Environ.* 7 (2005) 160–165.
- [35] K. Kover, Radiological constraints of using building materials and industrial by-products in construction, *Constr. Build. Mater.* 23 (2009) 246–253.
- [36] J. Somlai, V. Jobbágy, J. Kovács, S. Tarján, T. Kovács, Radiological aspects of the usability of red mud as a building material additive, *J. Hazard. Mater.* 150 (2008) 541–545.